ISSN 1063-7834, Physics of the Solid State, 2019, Vol. 61, No. 5, pp. 867–873. © Pleiades Publishing, Ltd., 2019.
Russian Text © The Author(s), 2019, published in Fizika Tverdogo Tela, 2019, Vol. 61, No. 5, pp. 960–966.

OPTICAL PROPERTIES

Synthesis and Luminescent Properties of Bismuth Titanates $Bi_{1.6}Ho_xTi_2O_{7-\delta}$ and $Bi_{1.6}Mg_{0.1}Ho_xTi_2O_{7-\delta}$

A. V. Ishchenko[a,*], M. S. Koroleva[b], M. I. Vlasov[a,c], E. I. Istomina[b], and I. V. Piir[b]

[a] *Ural Federal University Named after the First President of the Russia B.N. Yeltsin, Yekaterinburg, 620002 Russia*
[b] *Institute of Chemistry, Komi Scientific Center, Ural Branch, Russian Academy of Sciences, Syktyvkar, 167982 Russia*
[c] *Institute of High Temperature Electrochemistry, Ural Branch, Russian Academy of Sciences, Yekaterinburg, 620219 Russia*
**e-mail: a-v-i@mail.ru*

Received December 4, 2018; accepted December 5, 2018

Abstract—Pyrochlores $Bi_{1.6}Ho_xTi_2O_{7-\delta}$ and $Bi_{1.6}Mg_{0.1}Ho_xTi_2O_{7-\delta}$, where $x = 0$, 0.01, 0.05, and 0.1, and $Bi_{1.5}Ho_xTi_2O_{7-\delta}$, where $x = 0.25$ and 0.5, have been synthesized and their structural, optical, and luminescence properties have been studied. As a result of analyzing the data obtained experimentally and the available theoretical data, it is shown that the intrinsic luminescence of the samples is due to the O2*p* ↔ Bi6*p* and Bi6*s* ↔ Bi6*p* electron transitions and the impurity luminescence is due to the *f*–*f* transitions in Ho^{3+} and the O2*p* → Ho^{3+} charge transfer.

DOI: 10.1134/S1063783419050111

1. INTRODUCTION

Compounds with the pyrochlore structure of the $A_2^{3+}B_2^{4+}O_6O'$ have been known for a long time [1]. This structural type has been studied well and, according to recent concepts, is considered as a superposition of two interpenetrating sublattices A_4O' (anti-crystobalite type) and B_2O_6 skeleton from octahedra BO_6 connected by tips) [2]. Many compounds, among which bismuth titanate $Bi_2Ti_2O_7$ can be noted, crystallize in the pyrochlore structural type. In recent decades, the interest in this material has continuously increased, due to the number of its unique properties [2]. Bismuth titanates have relatively high dielectric permittivity, low dielectric losses, low synthesis temperatures, good electrical and luminescent properties of the compositions with rare-earth doping impurity, and, as a result, they can be used as materials for reservoir capacitors, luminophor composition for optical fibers, as efficient materials with the anti-Stokes luminescence, as luminescent markers for delivering drugs, etc. [2–4]. In this report, we present the results of the studies of the structural, optical, and luminescence properties in the visible spectral region upon the optical excitation and the cathode-beam excitation of bismuth titanate solid solutions $Bi_{1.6}Ho_xTi_2O_{7-\delta}$ and $Bi_{1.6}Mg_{0.1}Ho_xTi_2O_{7-\delta}$, where $x = 0$, 0.01, 0.05, and 0.10, and $Bi_{1.5}Ho_xTi_2O_{7-\delta}$, where $x = 0.25$ and 0.50.

2. EXPERIMENTAL

The substituted $Bi_{1.6}Ho_xTi_2O_{7-\delta}$ and $Bi_{1.6}Mg_{0.1}Ho_xTi_2O_{7-\delta}$ ($x = 0$, 0.1, 0.05) bismuth titanates have been synthesized by the solid-state reaction method from initial oxides Bi_2O_3 (99.99%), Ho_2O_3 (99.99%), MgO (99.99%), and TiO_2 (99.999%, anatase). The stoichiometric amount of the oxides were ground in a jaspar mortar for 30 min pressed into pellets ($d = 15$ mm, $h \sim 1.0$ mm), placed in corundum crucibles, and calcined at various temperatures T, °C (t, h): 650 (10), 850 (10), 950 (20), and 1000 (20) with the intermediate grinding of the samples. The further annealing temperature was varied within the range of 1100–1150°C (20 h) in the dependence on the composition.

The $Bi_{1.6}Ti_2O_{6.4}$ and $Bi_{1.6}Mg_{0.1}Ti_2O_{6.5}$ samples were synthesized by the co-precipitation method. The precursors were titanium tetraisopropilate $Ti(OC_3H_7)_4$, bismuth nitrate pentahydrate $Bi(NO_3)_3 \cdot 5H_2O$ (99.9%), and magnesium nitrate crystalline hexahydrate $Mg(NO_3)_2 \cdot 6H_2O$ (99.9%). The precursor masses were calculated to obtain 3 g of finished product. The stoichiometric amount of the crystallohydrates were dissolved in an aqueous solution of nitric acid (50 cm^3, 2.8 mol/dm^3) and added $Ti(OC_3H_7)_4$; added 30 cm^3 of concentrated ammonia solution; the obtained colloidal solution was mixed for 10 min, filtered, and washed with distilled water ($V(H_2O) = 1.2$ dm^3) to pH ≈ 7. The obtained precipitate was dried at 95°C (5 h) and calcined at 650°C (6 h).

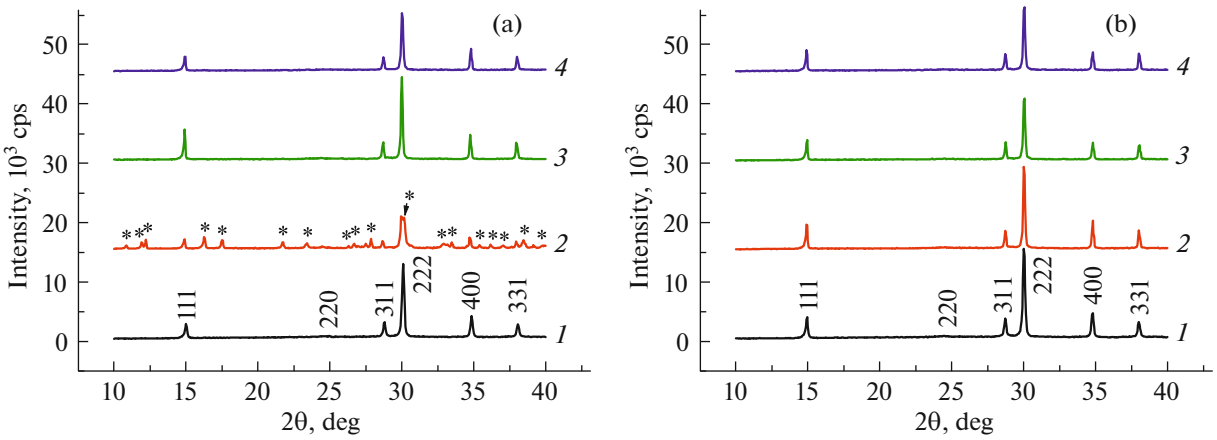

Fig. 1. X-ray diffraction patterns of (a) $Bi_{1.6}Ho_xTi_2O_{7-\delta}$ and (b) $Bi_{1.6}Mg_{0.1}Ho_xTi_2O_{7-\delta}$: $x =$ (*1*) 0, (*2*) 0.01, (*3*) 0.05, and (*4*) 0.1.

The phase compositions of the samples were studied by X-ray diffraction (XRD) analysis using on a SHIMADZU XRD-6000 diffractometer (CuK_α radiation, 10°–40°, step was 0.05°, the exposition time was 3 s) at 25°C. The local compositions of the phases in the samples were determined for mechanically polished ceramic surfaces using an X-ACT energy dispersive microanalyzer (EDS) combined with a TESCAN VEGA 3SBU scanning electron microscope (SEM). The micrographs of the samples were obtained in back-scattered electrons (BSE regime). The local compositions of the phases in the $Bi_{1.6}Ti_2O_{6.4}$ (BTO) and $Bi_{1.6}Mg_{0.1}Ti_2O_{6.5}$ (BTMO) were determined on the powders.

The optical diffuse reflectance spectra were measured at room temperature using a Shimadzu 2450 spectrometer with an ISR-2200 (300–900 nm) integrating sphere. $BaSO_4$ was used as a reference. The optical absorption spectra were obtained by the conversion of the diffuse reflectance spectra to function $F(R)$ proportional to the absorption coefficient by the Kubelka–Munk formula [5]: $F(R) = (1 - R)^2/2R$, where R is the diffuse reflectance coefficient.

The spectra of pulsed cathodoluminescence (PCL) were measured on a KLAVI-R apparatus (produced at IEPh, Ural Branch, RAS, Yekaterinburg) equipped with a RADAN (pulsed electron gun) (pulse duration 2 ns, electron energy 150 keV, the current density in a pulse 150 A/cm^2) and a luminescence recorder based on a CCD sensor with an electron–optical converter (the measurement range is 350–800 nm).

The photoluminescence (PL) and photoluminescence excitation (PLE) spectra were recorded on a Perkin Elmer LS-55 spectrophotometer using a pulsed xenon lamp and a Hamamatsu R928 FEU.

3. SAMPLE CRYSTAL STRUCTURE AND MORPHOLOGY

It was shown by the XRD and SEM methods that the pyrochlore structure ($Fd\bar{3}m$ space group, no. 227) forms at 650°C for $Bi_{1.6}Ho_xTi_2O_{7-\delta}$ and $Bi_{1.6}Mg_{0.1}Ho_xTi_2O_{7-\delta}$ at $x = 0$ and at 1100–1150°C as $x = 0.01$, 0.05, and 0.10. The solid-phase synthesis of the compositions with $x < 0.05$ at the bismuth-to-titanium molar proportion 1.6 : 2 leads to the formation of the more stable phase of layered perovskite $Bi_4Ti_3O_{12}$ (Fig. 1, additional phase is indicated by asterisk), which was caused by a narrow region of the stability of the pyrochlore structure $1.46 \le r(A)/r(B) \le 1.78$ ($A_2^3B_2^{4+}O_6O'$) [5]. According to [6–14], the pyrochlore structure forms in the $Bi_{1.6}M_xTi_2O_{7-\delta}$ (M = Cr, Fe, Mn, Co, In, Sc, and Li) system at $x \approx 0.05$–0.10.

The local compositions of the samples determined by the energy-dispersive microanalysis almost correspond to initial compositions (Table 1). Table 1 also gives the unit cell parameters for each of the samples. The SEM images for $Bi_{1.6}Ti_2O_{6.4}$ and $Bi_{1.6}Mg_{0.10}Ti_2O_{6.5}$ (Fig. 2) show that the samples consist of agglomerates with particles 100–300-nm in size.

4. OPTICAL AND LUMINESCENT PROPERTIES

The optical properties of the samples were studied by the diffuse reflectance spectroscopy. Figure 3 shows the diffuse reflectance spectra measured for a number of the BTO samples at various magnesium and holmium doping concentrations. One can see that the introduction of holmium leads to the appearance of several narrow absorption bands related to the electron excitations in ions Ho^{3+}. In this case, the addition of 5% Mg^{2+} (distributed in A(Bi) positions in the pyrochlore-type structure [12, 13]) only slightly affects the character of the spectra of the samples with hol-

Table 1. Results of the EDS analysis (SEM) of $Bi_{1.6}Ho_xTi_2O_{7-\delta}$ and $Bi_{1.6}Mg_{0.1}Ho_xTi_2O_{7-\delta}$

Composition	Composition by EDS (SEM)	Unit cell parameters, a, Å
$Bi_{1.6}Ti_2O_{6.4}$	$Bi_{1.66}Ti_2O_{-\delta}$	10.288(3)
*$Bi_{1.6}Ho_{0.01}Ti_2O_{6.415}$	–	10.325(4)
$Bi_{1.6}Ho_{0.05}Ti_2O_{6.475}$	$Bi_{1.66}Ho_{0.05}Ti_2O_{7-\delta}$	10.317(4)
$Bi_{1.6}Ho_{0.10}Ti_2O_{6.415}$	$Bi_{1.62}Ho_{0.10}Ti_2O_{7-\delta}$	10.303(3)
$Bi_{1.6}Mg_{0.10}Ti_2O_{6.5}$	$Bi_{1.65}Mg_{0.03}Ti_2O_{7-\delta}$	10.312(4)
$Bi_{1.6}Mg_{0.10}Ho_{0.01}Ti_2O_{6.515}$	$Bi_{1.68}Mg_{0.09}Ho_0Ti_2O_{7-\delta}$	10.312(3)
$Bi_{1.6}Mg_{0.10}Ho_{0.05}Ti_2O_{6.575}$	$Bi_{1.67}Mg_{0.08}Ho_{0.05}Ti_2O_{7-\delta}$	10.313(3)
$Bi_{1.6}Mg_{0.10}Ho_{0.10}Ti_2O_{6.65}$	$Bi_{1.63}Mg_{0.09}Ho_{0.10}Ti_2O_{7-\delta}$	10.310(4)

*Non-single-phase sample.

mium and without it. To estimate the optical band gap width E_g, the spectra were transformed using the Kubelka–Munk formula to the spectra proportional to the optical absorption, and then Tauz approximation of indirect allowed transitions was applied (Fig. 4). In the undoped BTO, the value of E_g is approximately 3.0 eV and it insignificantly decreases as the Ho^{3+} dopant concentration increases (2.90, 2.84, and 2.83 eV for $x = 0.01$, 0.05, and 0.10, respectively). In the sample doped with Mg^{2+} ions, the optical gap width E_g increases insignificantly to ≈3.05 eV. The combined doping of BTO with holmium and magnesium (Ho^{3+} and Mg^{2+}) does not lead to substantial change in the lattice parameter (Table 1). In these compositions, the value of E_g is near 2.89–2.90 eV and is independent of the Ho^{3+} concentration. In [15, 16], it was shown that the activation of various oxides (in particular, ZnO) with magnesium can lead to an increase in the optical band gap width. Thus, as a result of superposition of two opposite effects caused due to doping with holmium and magnesium and leading to the compensation of the unit cell sizes, the optical band gap width is retained to be 2.89–2.90 eV.

The studies of the properties of PCL of the $Bi_{1.6}Ho_xTi_2O_{7-\delta}$ and $Bi_{1.6}Mg_{0.1}Ho_xTi_2O_{7-\delta}$ samples show that the spectral luminescence composition in the range 400–800 nm (Figs. 5a, 5b) contains narrow bands typical to the f–f transitions in Ho^{3+} ions: the intense band at 536–550 nm ($^5F_4$, $^5S_2 \rightarrow {}^5I_8$) and a series of weak transitions at 460–470 nm ($^5F_3 \rightarrow {}^5I_8$), 650–670 nm ($^5F_5 \rightarrow {}^5I_8$), and 770–780 nm ($^5I_4 \rightarrow {}^5I_8$). The maximum PCL intensity is observed in the samples with 0.1 at % Ho^{3+} ($x = 0.1$), which is well seen in the dependence of the luminescence intensity on the activator concentration (Fig. 5c). In addition to the narrow PCL lines of the bismuth titanates, a weak broad luminescence band with a maximum near 500 nm is observed in the spectra. This band can be ascribed to the luminescence of intrinsic luminescence centers, for example, the luminescence centers

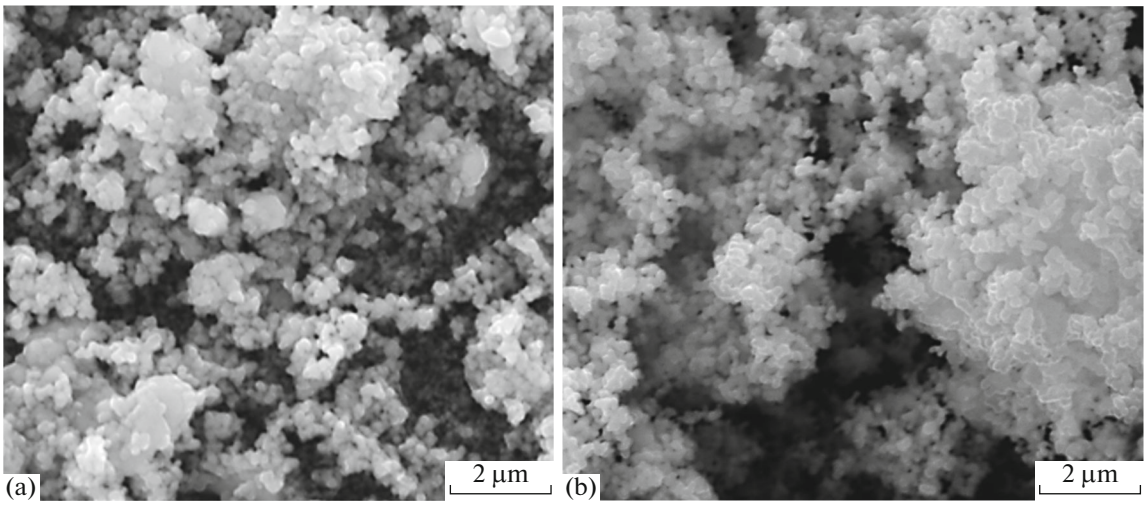

Fig. 2. SEM images for (a) $Bi_{1.6}Ti_2O_{6.4}$ and (b) $Bi_{1.6}Mg_{0.10}Ti_2O_{6.5}$.

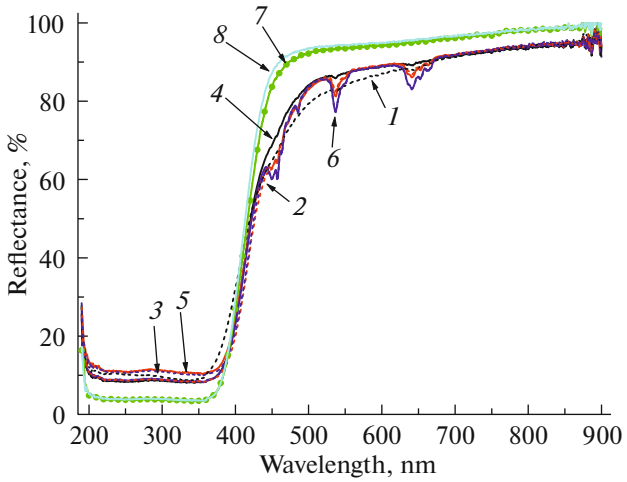

Fig. 3. Diffuse reflectance spectra of $Bi_{1.6}Ho_xTi_2O_{7-\delta}$ and $Bi_{1.6}Mg_{0.1}Ho_xTi_2O_{7-\delta}$: (*1*) $Bi_{1.6}Ho_{0.01}Ti_2O_{6.45}$, (*2*) $Bi_{1.6}Ho_{0.05}Ti_2O_{6.475}$, (*3*) $Bi_{1.6}Ho_{0.10}Ti_2O_{6.55}$, (*4*) $Bi_{1.6}Mg_{0.1}Ho_{0.01}Ti_2O_{6.51}$, (*5*) $Bi_{1.6}Mg_{0.1}Ho_{0.05}Ti_2O_{6.575}$, (*6*) $Bi_{1.6}Mg_{0.1}Ho_{0.10}Ti_2O_{6.65}$, (*7*) $Bi_{1.6}Ti_2O_{6.4}$, and (*8*) $Bi_{1.6}Mg_{0.1}Ti_2O_{6.5}$.

related to Bi^{3+} ions or defects in the oxygen sublattice; however, additional analysis of this band is hampered because of low luminescence intensity. As can be seen from the PCL spectra, the introduction of Mg^{2+} ions to the bismuth titanate compositions does not lead to a marked change in the luminescence spectra (Figs. 5a, 5b).

The PLE and PL spectra of all these bismuth titanates activated with Ho^{3+} are similar to each other. The introduction of coactivator Mg^{2+} does not change the shapes of the PL and PLE spectra. We failed to study the photoluminescence properties of the samples without Ho^{3+} because of low luminescence intensity. Figure 6 shows, as an example, the PL and PLE spectra of the $Bi_{1.5}Ho_{0.1}Ti_2O_{7-\delta}$ sample; these data will be used for further analysis.

The PL spectrum excited by a light with wavelength 455 nm has a smaller number of bands as compared to the PLE spectrum. An intense line is clearly observed near 536–550 nm ($^3F_4$, $^5S_2 \rightarrow {}^5I_8$). This difference is related to lower efficiency of excitation of PL than that of PCL.

The PLE spectrum was measured for the luminescence band at 536–550 nm (transition $^3F_4$, $^5S_2 \rightarrow {}^5I_8$ in Ho^{3+}). As one can see, the spectrum consists of a series of intense narrow bands with maxima at 483, 470, 462, 457, 451, and 419 nm and broad low-intense bands with maxima at 360, 285, and 236 nm. The narrow bands can be ascribed to the intracenter transitions in Ho^{3+} ions. Figure 6 demonstrates the ascription of the transitions to a specific band. The appearance of the bands with maxima near 545 nm (term ($^3F_4$, $^5S_2 \rightarrow {}^5I_8$)) both in the reflectance spectrum and in the PL spectrum indicates that these levels take part in the luminescence processes and also in the processes of the energy absorption with its subsequent release with participation of lower-laying $^5F_5$, $^5I_4$, $^5I_5$, $^5I_6$, and $^5I_7$ levels (the scheme of the levers is shown in Fig. 6b).

The appearance of the broad low-intensity bands can be related to the energy transfer from excited ions of the bismuth titanate matrix to activator Ho^{3+}. A possible reason is discussed below.

Additional information on the energy transfer processes in bismuth titanates with activator Ho^{3+} can be obtained by a combined analysis of the PLE and PL spectra, the diffuse reflectance and absorption spectra (Fig. 6). It is seen from Fig. 6, that the region of the fundamental absorption in holmium-doped bismuth titanates is in the region of energies higher than 3.0 eV (less than 410 nm (Fig. 6, the absorption spectrum)). According to the results of the quantum-chemical simulation [17], performed for bismuth titanates with the pyrochlore structure doped with magnesium and calcium ($Bi_{1.5}Mg_{0.5}Ti_2O_7$ and $Bi_{1.5}Ca_{0.5}Ti_2O_7$), the valence band in these materials is predominantly formed due to 2*p* states of oxygen ions O^{2-} and 6*s* states of Bi^{3+} ions. The Bi^{3+} ion states are distributed over the first valence band nonuniformly: the 6*s* states lie close to the Fermi level, and the 6*p* states are almost 5 eV lower than the Fermi level. The conduction band is mainly formed due to 3*d* states of Ti^{4+} ions; however, in the low-energy part, there is a marked contribution of the Bi6*p* states. According to the calculation results [17], the contribution of the states of Mg^{2+} and Ca^{2+} ions to the formation of the valence band and the conduction band is very small; thus, the direct participation of these activators in the luminescence processes is minimal. This theoretical result is confirmed experimentally. The data on PCL show that the introduction of Mg^{2+} ions to the BTO structure does not influence the spectral characteristics. Nevertheless, the introduction of the heterovalent impurity can lead to an increase in the point defect concentration in the BTO structure, which can lead to the formation of traps for charge carriers. This assumption needs additional studies using the thermoluminescence spectroscopy techniques. However, taking into account the low intensity of the luminescence of the samples, the performance of such experiments is quite difficult problem. From the analysis of the calculation results, it follows that the fundamental absorption in bismuth titanates (Fig. 6, the absorption spectrum) is mainly due to electron transitions $O2p \rightarrow Ti3d$ and, in a less degree, by the $Bi6s \rightarrow Bi6p$ transitions in bismuth ions and the $O2p \rightarrow Bi6p$ charge-transfer transitions. The comparison of the PLE spectra and the optical absorption spectra (Fig. 6) shows that the interband transitions in bismuth titanates do not lead to an

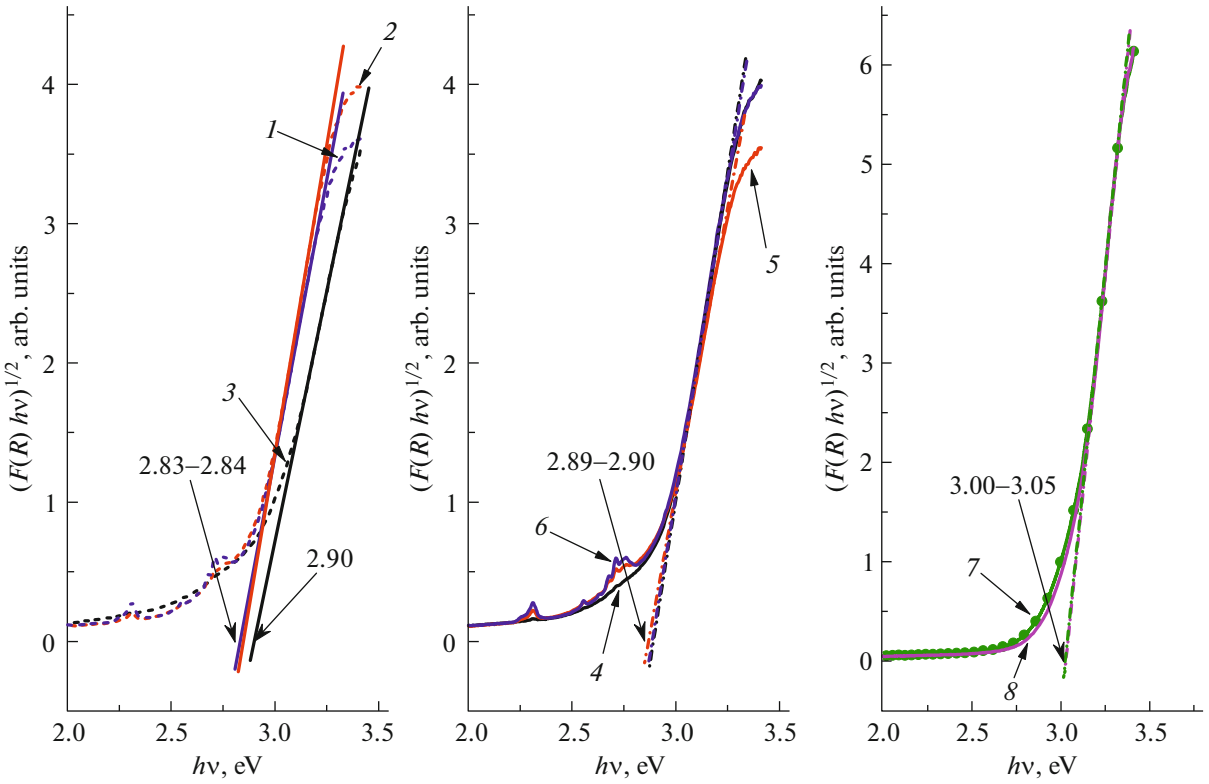

Fig. 4. Absorption spectra of bismuth titanate in the Tauz coordinates calculated in an approximation of indirect allowed transitions and the optical band gap widths for them: (*1*) $Bi_{1.6}Ho_{0.01}Ti_2O_{6.45}$, (*2*) $Bi_{1.6}Ho_{0.05}Ti_2O_{6.475}$, (*3*) $Bi_{1.6}Ho_{0.10}Ti_2O_{6.55}$, (*4*) $Bi_{1.6}Mg_{0.1}Ho_{0.01}Ti_2O_{6.51}$, (*5*) $Bi_{1.6}Mg_{0.1}Ho_{0.05}Ti_2O_{6.575}$, (*6*) $Bi_{1.6}Ho_{0.01}Ti_2O_{6.65}$, (*7*) $Bi_{1.6}Ti_2O_{6.4}$, and (*8*) $Bi_{1.6}Mg_{0.1}Ti_2O_{6.5}$.

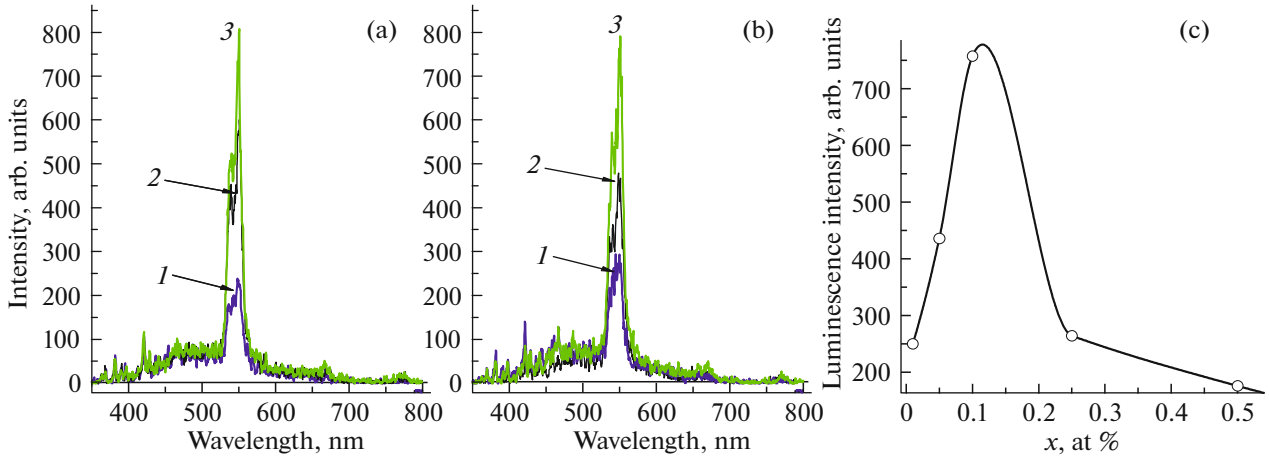

Fig. 5. PLE spectra of bismuth titanates (a) $Bi_{1.6}Ho_xTi_2O_{7-\delta}$ and (b) $Bi_{1.6}Mg_{0.1}Ho_xTi_2O_{7-\delta}$ and (c) the dependence of the luminescence intensity of the 545 nm band on the Ho^{3+} concentration: $x =$ (*1*) 0.01, (*2*) 0.05, and (*3*) 0.1.

intense luminescence, unlike, for example, the known $Bi_4Ge_3O_{12}$ (BGO) scintillator. In BGO, as the ab initio calculations show [18], the efficient excitation of the luminescence occurs due to the O2p → Bi6p and Bi6s → Bi6p electron transfers. The Ge4p states in BGO, unlike Ti3d in BTO, are not dominant during the formation of the conduction band and they are absent in its low-energy band. The intrinsic luminescence in BGO is due to the decay of electron excitations on Bi^{3+} ions. The intrinsic luminescence is

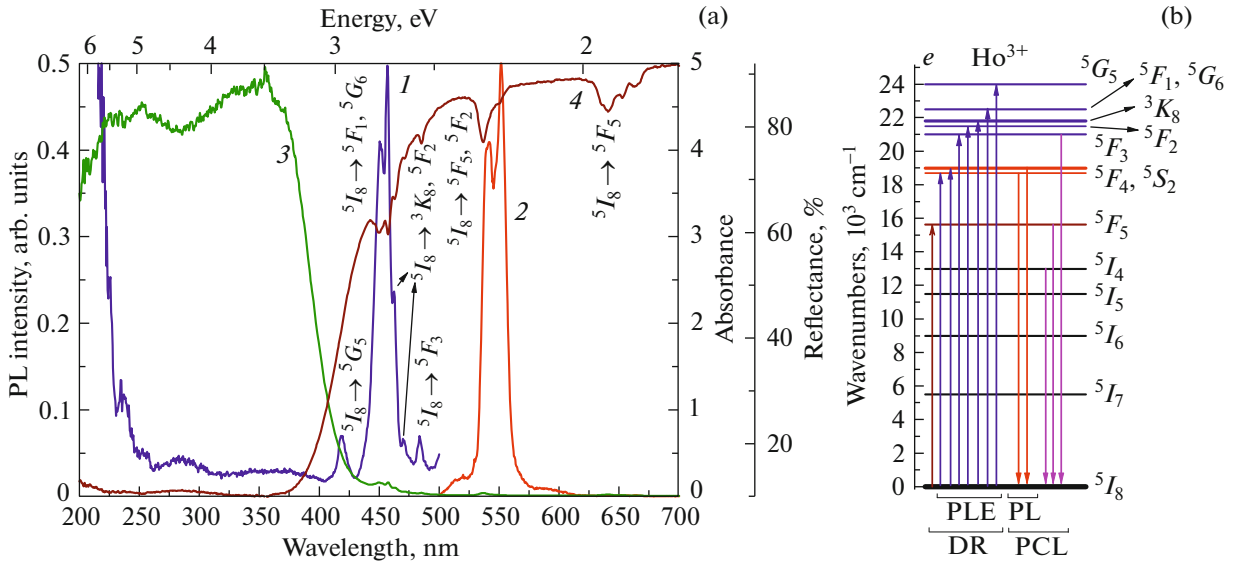

Fig. 6. (a) (*1*) PLE and (*2*) PL spectra, (*3*) absorption spectra, and (*4*) diffuse reflectance spectra of the $Bi_{1.5}Ho_{0.1}Ti_2O_{7-\delta}$ sample. The PLE spectrum was measured for the luminescence band at 545 nm; the PL spectrum was measured at the excitation by light with wavelength 455 nm. (b) Scheme of the observed electron transitions in Ho^{3+} ions in bismuth titanates. DR is for diffuse reflectance.

known to be almost absent in titanates with $[TiO_6]^{8-}$ matrix complexes [19]. This is related to the specific features of relaxation of electron excitations in the octahedral complexes containing a tetravalent metal. Complexes with pentavalent and hexavalent metals in the tetrahedral or octahedral coordination exhibit, as a rule, intense luminescence, for example: vanadates, tungstate molybdates, etc. The octahedral and tetrahedral complexes with titanium usually act as efficient luminescence centers if they are introduced in a wide-gap crystal as an impurity. In the case of BTO, we observe the intense light absorption by the $[TiO_6]^{8-}$ groups in the range 200–400 nm (Fig. 6, the absorption spectrum) without subsequent luminescence at room temperature (transition O2$p \rightarrow$ Ti3d) and a weak intrinsic luminescence due to the O2$p \rightarrow$ Ti3d and Bi6$s \rightarrow$ Bi6p electron transitions (broad low-intense bands in the PLE spectrum with maxima at 360 and 285 nm (Fig. 6, the PLE spectrum)) in a bismuth polyhedron with the subsequent radiation relaxation. In BTO, the intrinsic luminescence is observed as a broad luminescence band in the PLE spectra with a maximum at 500 nm (Figs. 5a, 5b). As a result, we can conclude that the low intensity of the intrinsic luminescence related to polyhedrons with Bi^{3+} is due to the intense light absorption in the $[TiO_6]^{8-}$ complexes. For more detailed study of the processes related to the intrinsic luminescence in BTO, it is necessary to carry out low-temperature measurements.

At room temperature, the luminescence of Ho^{3+} ions in the bismuth titanates has two excitation channels. The first of them is related to the intracenter f–f transitions, which is well seen from the comparison of the PLE spectrum and the optical absorption spectrum (Fig. 6, the PLE spectrum and the absorption spectrum). The excitation of the luminescence band corresponding to the $^3F_4$, $^5S_2 \rightarrow {}^5I_8$ transition (536–550 nm) occurs due to the electron transfer from the ground $^5I_8$ level to the $^5G_5$, $^5F_1$, $^5G_6$, $^3K_8$, $^5F_2$, and $^5F_3$ levels lying in the energy gap of BTO. The higher-energy f–f transitions in Ho^{3+} ions are not realized because of the intense light absorption with an energy higher 3 eV by the $[TiO_6]^{8-}$ matrix complexes (O2$p \rightarrow$ Ti3d). Another channel of the Ho^{3+} luminescence excitation can be referred to the O2$p \rightarrow Ho^{3+}$ transition with charge transfer that is observed as the luminescence excitation band in the PLE spectrum with a maximum at 236 nm (Fig. 6, the PLE spectrum). A similar band is observed in La_2O_3:Ho^{3+} [20].

5. CONCLUSIONS

In this work, we have synthesized bismuth titanates doped with magnesium and holmium and studied their structural, optical, and luminescent properties. The samples have relatively low luminescence intensity. The maximum luminescence intensity was observed in the samples with the Ho^{3+} concentration equal to 0.1 at %. It is shown that the concentration of the Ho^{3+} ions in the pyrochlore-type structures in $Bi_{1.6}Ho_xTi_2O_{7-\delta}$ and $Bi_{1.6}Mg_{0.1}Ho_xTi_2O_{7-\delta}$, where $x =$ 0, 0.01, 0.05, and 0.1, and $Bi_{1.5}Ho_xTi_2O_{7-\delta}$, where $x =$ 0.25 and 0.5, weakly influences the unit cell volume and the optical band gap width. The introduction of

Mg^{2+} ions only slightly influences the luminescent properties of the bismuth titanates doped with holmium. As a result of analyzing the experimental data obtained in this work and the available theoretical data, we described the processes of generation and relaxation of electron excitations related to the intrinsic O2p → Bi6p and Bi6s → Bi6p electron transitions, and the impurity luminescence (f–f transitions in Ho^{3+} ions and the O2p → Ho^{3+} charge transfer) in these compounds.

FUNDING

The reported study was funded by RFBR according to the research project 19-03-00642.

REFERENCES

1. M. A. Subramanian, G. Aravamudan, and G. V. Subba Rao, Prog. Solid State Chem. **15**, 55 (1983).
2. F. Li, X. Liu, J. Zhao, L. Liu, Sh. He, and D. Bao, Mater. Chem. Phys. **162**, 801 (2015).
3. Y. Cun, Zh. Yang, J. Liao, J. Qiu, Zh. Song, and Y. Yang, Mater. Lett. **131**, 154 (2014).
4. X. N. Yanga, B. B. Huanga, H. B. Wangb, S. X. Shangc, W. F. Yaoa, and J. Y. Weia, J. Cryst. Growth **270**, 98 (2004).
5. P. Kubelka, J. Opt. Soc. Am. B **38**, 448 (1948).
6. I. V. Piir, N. A. Sekushin, V. E. Grass, Y. I. Ryabkov, N. V. Chezhina, S. V. Nekipelov, V. N. Sivkov, and D. V. Vyalikh, Solid State Ionics **225**, 464 (2012).
7. I. V. Piir, M. S. Koroleva, D. A. Korolev, N. V. Chezhina, V. G. Semenov, and V. V. Panchuk, J. Solid State Chem. **204**, 245 (2013).
8. M. S. Koroleva, I. V. Piir, Yu. I. Ryabkov, D. A. Korolev, and N. V. Chezhina, Russ. Chem. Bull. **62**, 408 (2013).
9. I. V. Piir, M. S. Koroleva, Y. I. Ryabkov, E. Y. Pikalova, S. V. Nekipelov, V. N. Sivkov, and D. V. Vyalikh, Solid State Ionics **262**, 630 (2014).
10. I. V. Piir, M. S. Koroleva, N. A. Sekushin, V. E. Grass, and Yu. I. Ryabkov, Russ. J. Electrochem. **49**, 817 (2013).
11. A. G. Krasnov, I. V. Piir, M. S. Koroleva, N. A. Sekushin, Y. I. Ryabkov, M. M. Piskaykina, V. A. Sadykov, E. M. Sadovskaya, V. V. Pelipenko, and N. F. Eremeev, Solid State Ionics **302**, 118 (2017).
12. A. G. Krasnov, M. M. Piskaikina, and I. V. Piir, Russ. J. Gen. Chem. **86**, 205 (2016).
13. A. G. Krasnov, M. M. Piskaikina, and I. V. Piir, Khim. Interesakh Ustoich. Razvit. **24**, 687 (2016).
14. V. A. Sadykov, M. S. Koroleva, I. V. Piir, N. V. Chezhina, D. A. Korolev, P. I. Skriabin, A. V. Krasnov, E. M. Sadovskaya, N. F. Eremeev, S. V. Nekipelov, and V. N. Sivkov, Solid State Ionics **315**, 33 (2018).
15. Y. S. Wang, P. J. Thomas, and P. O'Brien, J. Phys. Chem. B **110**, 21412 (2006).
16. F. K. Shan, B. I. Kim, G. X. Liu, Z. F. Liu, J. Y. Sohn, W. J. Lee, and B. C. Shin, J. Appl. Phys. **95**, 4772 (2004).
17. A. G. Krasnov, I. R. Shein, I. V. Piir, and Y. I. Ryabkov, Solid State Ionics **317**, 183 (2018).
18. A. F. Lima, S. O. Souza, and M. V. Lalić, J. Appl. Phys. **106**, 013715 (2009).
19. G. Blasse, *Luminescence and Energy Transfer*, Vol. 42 of *Structure and Bonding* (Springer, Berlin, Heidelberg, 1980).
20. G. Li, Ch. Li, Zh. Xu, Z. Cheng, and J. Lin, Cryst. Eng. Commun. **12**, 4208 (2010).

Translated by Yu. Ryzhkov